INFLUENCE OF PHYSICAL FORCING ON
CARBON MICROCLOUDS IN THE OCEAN

B. J. Rothschild
P.J. Haley, Jr.

May 2, 1996

REPORT DOCUMENTATION PAGE

Public reporting burden for this collection of information is estimated to average 1 hour per response, including the time for reviewing instructions, searching existing data sources, gathering and maintaining the data needed, and completing and reviewing the collection of information. Send comments regarding this burden estimate or any other aspect of this collection of information, including suggestions for reducing this burden, to Washington Headquarters Services, Directorate for Information Operations and Reports, 1215 Jefferson Davis Highway, Suite 1204, Arlington, VA 22202-4302, and to the Office of Management and Budget, Paperwork Reduction Project (0704-0188), Washington, DC 20503.

1. AGENCY USE ONLY (Leave blank)	2. REPORT DATE 2 May 96	3. REPORT TYPE AND DATES COVERED Final 1 Jul 92 to 30 Apr 95

4. TITLE AND SUBTITLE Influence of Physical Forcing on Carbon Microclouds in the Ocean	5. FUNDING NUMBERS G N00014-92-J-4070

6. AUTHOR(S)

B. J. Rothschild
P. J. Haley, Jr.

7. PERFORMING ORGANIZATION NAME(S) AND ADDRESS(ES) University of Maryland Center for Environmental and Estuarine Studies (Chesapeake Biological Laboratory) P.O. Box 775 Cambridge, Maryland 21613	8. PERFORMING ORGANIZATION REPORT NUMBER None

9. SPONSORING/MONITORING AGENCY NAME(S) AND ADDRESS(ES) Office of Naval Research Atlanta Regional Office Atlanta, Georgia 30323-0008	10. SPONSORING/MONITORING AGENCY REPORT NUMBER

11. SUPPLEMENTARY NOTES

12a. DISTRIBUTION/AVAILABILITY STATEMENT Unlimited	12b. DISTRIBUTION CODE

13. ABSTRACT (Maximum 200 words)

The transformation of DOC into heterotrophic biomass is an important ecological pathway. This paper studies the theoretical basis for variability in the transformation resulting from aggregations of DOC microzones or microclouds. The paper computes measures of aggregation using the theory of stochastic geometry. The theory enables computation of aggregation in terms of the volume fraction occupied by microclouds and computation of length scales such as covariance functions and spherical contact distributions. Using real data on phytoplankton cell density and size, and conjectured dimensions of microzones, we were able to compute the volume fraction, covariance functions and spherical contact distributions for assembleges of Baltic Sea phytoplankton. By comparing microcloud length scales with molecular diffusion, turbulent diffusion and uncorrelated velocity length scales we determined that variability in the turbulent kenetic energy dissipation rate, which might be induced by global and basin scale wind forcing (for example), could influence the geometric structure of carbon microclouds. This demonstrates the plausibility of linking the largest scale physical forcing directly to the microscale structure when considering variability in the transformation of primary to secondary production.

14. SUBJECT TERMS Dissolved Organic Carbon (DOC) Primary Production Heterotrophic Biomass Secondary Production Aggregation Theory	15. NUMBER OF PAGES 19
	16. PRICE CODE

17. SECURITY CLASSIFICATION OF REPORT unclassified	18. SECURITY CLASSIFICATION OF THIS PAGE. unclassified	19. SECURITY CLASSIFICATION OF ABSTRACT unclassified	20. LIMITATION OF ABSTRACT UL

NSN 7540-01-280-5500

Standard Form 298 (Rev. 2-89)
Prescribed by ANSI Std. 239-18

Influence of Physical Forcing on Carbon Microclouds in the Ocean

B.J. Rothschild and P.J. Haley Jr.

May 2, 1996

0.0 Abstract

The transformation of DOC into heterotrophic biomass is an important ecological pathway. This paper studies the theoretical basis for variability in the transformation resulting from aggregations of DOC microzones or microclouds. The paper computes measures of aggregation using the theory of stochastic geometry. The theory enables computation of aggregation in terms of the volume fraction occupied by microclouds and computation of length scales such as covariance functions and spherical contact distributions. Using real data on phytoplankton cell density and size, and conjectured dimensions of of microzones, we were able to compute the volume fraction, covariance functions and spherical contact distributions for assembledges of Baltic Sea phytoplankton. By comparing microcloud length scales with molecular diffusion, turbulent diffusion and uncorrelated velocity length scales we determined that variability in the turbulent kenetic energy dissipation rate, which might be induced by global and basin scale wind forcing (for example), could influence the geometric structure of carbon microclouds. This demonstrates the plausibility of linking the largest scale physical forcing directly to the microscale structure when considering variability in the transformation of primary to secondary production.

1.0 Introduction

An important component of oceanic primary-secondary production transformation involves the absorption of dissolved organic carbon (DOC) by bacteria. There are several sources of variability associated with this transformation. One source of variability involves the fraction of total DOC absorbed as exudates at relatively high DOC concentrations very close to the photosynthesizing phytoplankton cells. This paper develops a theory on the spatial distribution of DOC in the proximity of phytoplankton cells. The theory generalizes the microzone model of bioactive DOC distribution near metabolizing planktonic organisms (see Mitchell *et al.*, 1985). In the microzone model, exuded-carbon molecules are concentrated in a spherical zone centered on each phytoplankton cell. The

1

**Center for Environmental
and Estuarine Studies**

University of Maryland System
Post Office Box 775
Cambridge, Md 21613
(410) 228-9250
FAX: (410) 228-3843

Center Operations
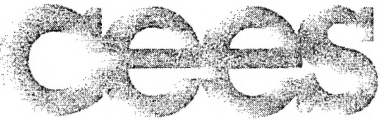
Celebrating Twenty Years of Discovery
1973 - 1993

May 8, 1996

Ms. Natalie V. Bryant
Procurement Technician
Department of the Navy
Office of Naval Research
Atlanta Regional Office
101 Marietta Tower
101 Marietta Street, Suite 2805
Atlanta, Georgia 30323-0008

Dear Ms. Bryant:

Enclosed is one copy of the final technical report for grant N00014-92-J-4070. This report has
been distributed in accordance with the terms of the grant.

Do not hesitate to contact us should you have any questions or require additional information.

Very truly yours,

Phyllis Rhoades
Contract Administrator

pir

Enclosure

cc: Dr. Bernard Zahuranec (Scientific Officer)
    Mr. Barry Copeland (Grants Officer)
    Naval Research Laboratory
    Defense Technical Information Center

concentration of molecules is highest at the cell wall and then declines according to the laws of molecular diffusion. The spherical zones are thought of as phycospheres or microzones (The idea of a phycosphere evidently originated in Bell and Mitchell, 1972).

However, in this paper we postulate that the microzones tend to intersect as the numerical density of the phytoplankton cells increases. A particular set of intersecting microzones can be thought of as a "microcloud". The ensemble of single microzones and microclouds comprises the microcloud structure–essentially different than the microzone structure–of DOC. Because microclouds are larger than microzones, they are subject to different modalities and intensity of physical forcing. The following sections of the paper discuss the theory, how it is applied and a specific example.

2.0 Theory

Using the calculus of stochastic geometry (see Stoyan *et al.*, 1987; Cressie, 1993; and Rothschild, 1992), the concentration and length-scale properties of microclouds can be derived as a special case of the general Boolean model. The model enables computation of the volume fraction, concentration factor, covariance function and spherical contact distribution of the microclouds. The volume fraction and the concentration factor statistics are measures of the influence of microclouds on DOC concentration while the covariance function and the spherical contact distribution are probability distributions reflecting microcloud length scales.

These statistics and distributions are developed from the general theory by assuming: (1) that the phytoplankton cells are distributed in $\Re^3$ according to the Poisson distribution with intensity λ and (2) that the radii of the microzones are distributed log-normally with mean, ξ, and variance, σ^2. Accordingly, the probability density function, f, of the radii is

$$f\left(r; \xi, \sigma^2\right) = \frac{\alpha}{\xi\sqrt{2\pi\ln\left(\alpha\right)}} \exp\left\{-\frac{\ln^2\left[\frac{r}{\xi}\alpha^{\frac{3}{2}}\right]}{\ln\alpha^2}\right\} \tag{1a}$$

where $\exp\left\{\cdot\right\}$ is the exponential function and

$$\alpha = \frac{\sigma^2}{\xi^2} + 1 \quad . \tag{1b}$$

The *volume fraction, p*, occupied by the *ensemble* of microclouds is,

$$p = 1 - e^{-\frac{4}{3}\pi\lambda\xi^3\alpha^3} \quad . \tag{2}$$

2

The volume fraction described in equation (2) allows for the possibility that the microzones intersect one another. The intersection of microzones can serve to enhance DOC concentrations in the microcloud over those in a microzone. An upper bound for this concentration effect can obtained by assuming an average concentration of carbon molecules within the sphere, so the *concentration factor*, C_f, is the ratio of the volume fraction without overlap to the actual volume fraction:

$$C_f = \frac{\frac{4}{3}\pi\lambda\xi^3\alpha^3}{p} \quad . \tag{3}$$

The concentration factor achieves its maximum value when the volume fraction without overlap is one. This yields a maximum value of $C_{f_{\max}} = \left(1 - e^{-1}\right)^{-1} \approx 1.58$.

The length scale for the statistical "size" of the average microcloud can be derived from the stochastic-geometry *covariance function*. The covariance, $C(\mathcal{R})$, is the probability that <u>both</u> the head and tail of a vector of length $\mathcal{R}$ are located within the volume occupied by the microclouds. Since this will be most often accomplished by having the vector within a single microcloud, the covariance can be thought of as indicating the average size of the microclouds. Very small vectors have a relatively high probability, p, of being contained within the average microcloud, while large vectors haver a lower probability, p^2, of being contained within the microcloud. The covariance function is given by,

$$C(\mathcal{R}) = p^2 + (1-p)^2 \left\{ e^{\frac{4}{3}\pi\lambda\left[\left\langle r^3 H\left(r-\frac{\mathcal{R}}{2}\right)\right\rangle - \frac{3}{2}\mathcal{R}\left\langle r^2 H\left(r-\frac{\mathcal{R}}{2}\right)\right\rangle + \frac{1}{16}\mathcal{R}^3\left\langle H\left(r-\frac{\mathcal{R}}{2}\right)\right\rangle\right]} - 1 \right\} \tag{4a}$$

where $\langle \cdot \rangle$ denotes an expected value defined by

$$\langle \cdot \rangle = \int_0^\infty (\cdot)\, f\left(r; \xi, \sigma^2\right)\, dr \quad , \tag{4b}$$

$$H(r) = \begin{cases} 1 & r > 0 \\ 0 & r < 0 \end{cases} \quad , \tag{4c}$$

and, for the log-normal distribution

$$\left\langle r^n H\left(r - \frac{\mathcal{R}}{2}\right)\right\rangle = \begin{cases} \frac{\xi^n}{2}\alpha^{\frac{n(n-1)}{2}}\operatorname{erfc}(\Delta) & \text{if} \quad \mathcal{R} \geq 2\xi\alpha^{n-\frac{1}{2}} \\ \frac{\xi^n}{2}\alpha^{\frac{n(n-1)}{2}}[1 + \operatorname{erf}(-\Delta)] & \text{if} \quad \mathcal{R} \leq 2\xi\alpha^{n-\frac{1}{2}} \end{cases} \tag{4d}$$

in which

$$\Delta = \frac{\ln\left[\frac{\mathcal{R}}{2\xi}\alpha^{\frac{3}{2}}\right]}{\sqrt{2\ln(\alpha)}} - \frac{n+1}{\sqrt{2}}\sqrt{\ln(\alpha)} \quad . \tag{4e}$$

3

A convenient rescaling of the covariance function is given by the *correlation function*:

$$\kappa(\mathcal{R}) = \frac{C(\mathcal{R}) - p^2}{p(1-p)} \quad .$$ (5)

Clearly, $\kappa \in [0, 1]$ with $\kappa = 1$ for perfect correlation and $\kappa = 0$ for zero correlation. This makes for easy comparisons of cases with different volume fractions, as well as corresponding with standard conventions for the notion of correlation.

The probability that a point selected at random from *outside* the volume occupied by the microclouds is within a distance $\mathcal{R}$ of a microcloud is given by the *spherical contact distribution*, $H_s(\mathcal{R})$, which, under our assumptions, is given by

$$H_s(\mathcal{R}) = 1 - e^{-\frac{4}{3}\pi\lambda\left[3\mathcal{R}\left(\sigma^2 + \xi^2\right) + 3\mathcal{R}^2\xi + \mathcal{R}^3\right]} \quad .$$ (6)

3.0 Application

In order to place equations (1)-(6) in the context of the DOC microcloud problem, we need to make choices for λ, ξ, σ^2 and $\mathcal{R}$. For purposes of demonstration, size-binned particle counter data from the Baltic sea were used (Kahru *et al.*, 1991). These size binned, or size frequency, data were used to compute estimates of the *numerical* cell density, λ and the lognormal parameters ξ and σ^2. The intensity, λ, ranges between $[10^3, 5\left(10^3\right)]$ $\left(\text{cells} \cdot \text{cm}^{-3}\right)$. These spatially averaged concentrations probably represent much higher local concentrations because of the known non-random distribution of phytoplankton cells.

With respect to the mean radius of the microzone, ξ, direct measurements have not been made (Mitchell *et al.*, 1985, have conjectured microzone dimensions and experiments have demonstrated the existance of (pH) microzones, Richardson and Stolzenbach, 1995). The theory of diffusion can, however, be used to approximate the microzone radius. It is well known that the steady state concentration of molecules diffusing away from a cell of radius r_{cell} is given by

$$c(r) = c_\infty + \left(c_{\text{cell}} - c_\infty\right)\frac{r_{\text{cell}}}{r}$$ (7)

where c_{cell} is the concentration at the cell wall and c_∞ is the far-field (or background) concentration. The microzone associated with the phytoplankton cell is that sphere within which the concentration exceeds a threshold value, $c_{\text{threshold}}$. We choose the threshold concentration such that the difference $(c_{\text{threshold}} - c_\infty)$ is a fixed fraction, δ, of the difference

4

$(c_{\text{cell}} - c_\infty)$. The mean radius is chosen to be that radius at which the concentration has fallen to $c_{\text{threshold}}$. That is, find ξ such that

$$c(\xi) = c_{\text{threshold}} \qquad (8)$$
$$= c_\infty + \delta\left(c_{\text{cell}} - c_\infty\right) \quad .$$

Using (7), this gives the mean radius as

$$\xi = \frac{r_{\text{cell}}}{\delta} \quad . \qquad (9)$$

In this paper we consider $\delta = 0.1$ which gives a microzone radius 10 times that of the phytoplankton cell. Fitting the Kahru *et al.* data to log-normal distributions via a χ^2 functional shows the mean phytoplankton cell radius to fall in the range $r_{\text{cell}} \in \left[4\left(10^{-4}\right),\ 8\left(10^{-4}\right)\right]$ cm. This corresponds to a mean microzone radius in the range

$$\xi \in \left[4\left(10^{-3}\right),\ 8\left(10^{-3}\right)\right] \text{cm} \quad . \qquad (10)$$

The magnitude of the variance in the microzone radii can arise either from the variability of the phytoplankton cell radii or from a lack synchrony of in exudation time. For the Kahru *et al.* data, the variance is found to lie in the range:

$$\sigma^2 \in \left[0.5\xi^2,\ 0.9\xi^2\right] \subset \left[8\left(10^{-6}\right),\ 6\left(10^{-5}\right)\right] \text{cm}^2 \quad . \qquad (11)$$

The variance and the mean, of course, specify the shape of the log-normal distribution.

The correlation function and the spherical contact distribution both depend upon an additional length interval, $\mathcal{R}$ (either a correlation distance or a distance to the nearest cloud). The range of $\mathcal{R}$ is determined by the questions being asked. We wish to examine the effect of physical processes (i.e. turbulence) on the microcloud structure. In particular, we consider the Kolmogorov length scale, η, and the turbulent scalar diffusion length scale, η_s. The Kolmogorov length scale is the smallest length scale on which the velocities are uncorrelated, while the turbulent scalar diffusion length scale is the smallest length scale at which the Kolmogorov eddies can strain a tracer. For the ocean, typical ranges for the Kolmogorov and turbulent scalar diffusion length scales are $\eta \in [0.1, 1.0]$ cm and $\eta_s \in \left[10^{-3}, 0.1\right]$ cm (the lowest values of the Kolmogorov and turbulent scalar diffusion length scale ranges correspond to more energetic cases). The length interval, $\mathcal{R}$, is then chosen to contain these ranges:

$$\mathcal{R} \supset \left[10^{-3},\ 1\right] \text{cm} \quad . \qquad (12)$$

4.0 Results

4.1 Estimates of Baltic phytoplankton statistical geometry parameters.

Fitting the Kahru *et al.* data to the log-normal distribution results in the curves of figure 1. The modal microzone radii fall in the range of $[23, 33]$ μm. The curves themselves span the range of those with small variability in radii to those with larger variability. As a general trend, the populations with larger radial variability are those with larger modal radii.

The resulting statistics are more conveniently displayed in terms of nondimensional variables. Noting that, on average, the volume occupied by one particle is λ^{-1}, then a sphere with this volume will have a radius, R_λ, given by

$$R_\lambda = \sqrt[3]{\frac{3}{4\pi\lambda}} \quad . \tag{13}$$

The mean, ξ, and length interval, $\mathcal{R}$, are nondimensionalized by dividing by R_λ. The variance, σ^2, is nondimensionalized by dividing by R_λ^2.

Figure 2 shows the volume fraction as a function of the relative mean radius, $\frac{\xi}{R_\lambda}$, and the relative variance, $\frac{\sigma^2}{R_\lambda^2}$. Circles are used to indicate the locations in parameter space of the Kahru *et al.* data, with a bounding region for the data shaded. The vertices of the bounding region are labelled (a)–(d) for comparison with figures 3–5. The volume fraction occupied by this Baltic data ranges from 0.1% to 10%.

Figure 3 displays the concentration factor as a function of the relative mean radius, $\frac{\xi}{R_\lambda}$, and the relative variance, $\frac{\sigma^2}{R_\lambda^2}$. The circles and shaded region are exactly the same as in figure 2. The concentration effect in the shaded region is bounded between a 0.03% increase and a 3% increase. This reflects that there is relatively little overlap in the Baltic phytoplankton population.

Figure 4 displays contours of the correlation function as a function of the relative length, $\frac{\mathcal{R}}{R_\lambda}$, and the relative mean radius, $\frac{\xi}{R_\lambda}$. The variance is held equal to half the mean radius squared in figure 4a, and equal to 0.9 times the mean radius squared in figure 4b. Both figures show a maximum in the correlation as a function of the relative mean radius. In figure 4a, the maximum occurs at about $\frac{\xi}{R_\lambda} = 0.70$, while in figure 4b the maximum shifts down to around $\frac{\xi}{R_\lambda} = 0.55$.

Figure 5 displays contours of the spherical contact distribution as a function of the relative separation, $\frac{\mathcal{R}}{R_\lambda}$, and the relative mean radius, $\frac{\xi}{R_\lambda}$. The variance is held equal to

half the mean radius squared in figure 5a, and equal to 0.9 times the mean radius squared in figure 5b. For small relative mean radius, $\frac{\xi}{R_\lambda} \ll 1$, the contours in both figures appear independent of the relative mean radius. In fact this region corresponds to mean radii so small that the spherical contact distribution essentially "sees" dimensionless points. As the relative mean radius increases, the contours tilt to the left, making it easier to be within a given distance of the microclouds. Although it is hard to see, the contours in figure 5b, $(\sigma^2 = 0.9\xi^2)$, tilt more than those in figure 5a, $(\sigma^2 = 0.5\xi^2)$. As a particular example, in figure 5a the contour $H_s(\mathcal{R}) = 0.9$ intersects the top, $\frac{\xi}{R_\lambda} = 10$, at a relative separation of $\frac{\mathcal{R}}{R_\lambda} = 0.005$, while in figure 5b the intersection occurs at $\frac{\mathcal{R}}{R_\lambda} = 0.004$.

4.2 Influence of physical processes on Baltic phytoplankton.

The length scales (the correlation function and the spherical contact distribution) of the microzones are roughly in the molecular diffusion, turbulent diffusion and Kolmogorov uncorrelate velocity length scales. The molecular diffusion length scale is not subject to variability in the turbulent kinetic energy dissipation rate, ϵ. However, both the turbulent diffusion and the Kolmogorov uncorrelated velocity length scales are subject to variations in ϵ. Oversimplistically, it is well known that ϵ in the upper ocean varies with the velocity of the wind field etc. This means that variations in the global wind field affect ϵ, and so it is important to determine whether the global wind field potentially affects the pathways by which DOC exuded by phytoplankton cells is converted into secondary production.

In order to judge the plausibility of the linkage between physical forcing and the microcloud length scales we have constructed rectangle in figures 4 and 5 that delimit the molecular diffusion, turbulent diffusion and turbulent velocity length scales.

In figure 4, we can see that microclouds are generally subject to molecular diffusion and the straining of the fluid that results from turbulent diffusion. On the other hand we can also see that the microclouds are not subject to forcing by uncorrelated velocities. This interpretation is distinct from the viewpoint that only microzones exist because microzones are only subject to molecular diffusion.

In figure 5, we see that the interaction between points in the void space and material inside the microzone is influenced by both turbulent diffusion and uncorrelated velocities, hence the interaction is affected by variability in ϵ. The significance of the effect of turbulent diffusion might involve the intensity of microcloud blending in a dynamic setting; while the significance of the effect of uncorrelated velocities is that there would be increases in encounter rates between particles not in a cloud and particles in a cloud

(see Rothschilde and Osborn, 1988). This would mean that encounters between secondary producers, especially microzooplankton, and bacteria feeding on DOC in or near a cloud could be enhanced or, more importantly, vary with, for example, the velocity of the wind field.

5.0 Discussion

5.1 The role of microclouds in regulating production.

The microcloud landscape is an important source of variability in regulating the coupling between primary and secondary production. The notion of the microcloud suggests that the DOC available to bacteria may be higher than might be assumed taking account of only some background level of carbon. In addition the rich variability in spatial distribution implies that spatial distribution is an important source of the variability in the primary to secondary production via the bacterial pathway.

The nature of the spatial coupling might be best thought of in terms of an initial random distribution of bacteria. Such a distribution might exist if carbon molecules were distributed at random. However, the microzone or microcloud notion ensures a non-random distribution of carbon molecules. As a result of possible tactic responses and accelerated growth rates in the regions of relatively high carbon molecule concentration it can be expected that the densities of bacteria in the microclouds would be higher than outside the microclouds. Thus high volume fractions would be conducive to a higher transfer rate between primary production and secondary production.

An alternative view of this coupling is presented in the work of Bowen *et al.* (1993). In their simulations a single phytoplankton cell was centered in the computational volume and 1000 bacteria were initially randomly placed around it. A time varying shear was imposed on the fluid, representing the shear induced by turbulence. Their results show that, although an individual bacterium could not remain in the neighborhood of a phytoplankton cell, their transient proximity was sufficient to give significantly enhanced exposures to exudates. This could be a very important mechanism for the Baltic sea populations, were the contact distribution shows that it is very easy to be close to a microcloud.

It would follow that higher concentration of bacteria in microzones would induce higher concentrations of microzooplankton and protists that feed upon bacteria. In strengthing the coupling to an even greater degree, the increased densities of the microzooplankton would also result from tactic respones and increased growth rates which are known to be exceptionally high with abundant food resources (e.g. Fenchel 1988).

8

The aggregation of a variety of small heterotrophs within the microcloud of carbon molecules suggests than the carbon microcloud is juxtaposed with an ammonium microcloud produced by the heterotrophs, closing the feedback loop and increasing to yet a greater degree the strength of the coupling. The synergy of this coupling would have the effect of enhancing phytoplankton growth through the increased availability of nutrients

This clearly evokes a very complex structure. On one hand, from the phytoplankton's point of view, the carbon gradients both overlap and decrease with distance from the cell wall. On the other hand, because of diffusion, the ammonium molecules increase in concentration with distance from the phytoplankton cell wall. Thus, from the phytoplankton's point of view, the environment consists of both a positive and a negative microcloud. The reverse is, of course, true from the heterotroph perspective.

5.2 Negative microclouds.

The negative microcloud is particularly important because its existance impacts upon the issue of diffusion limited nutrient availability for phytoplankton cells. Munk and Riley (1952) and Pasciak and Gavis (1974) have studied this problem in the context of molecular diffusion. Lazier and Mann (1989) observed that molecular diffusion is influenced at very small scales by turbulent flow and hence follows turbulent diffusion at very small scales. To some extent, variable concentration may be "smoothed" by strain resulting from turbulent flow. At any rate, all of the above results need to be modified by the existance of negative microclouds. In effect, the negative microcloud generates a structure of rather complex gradients and hence complex diffusional flux. In fact, it is possible for nutrient molecules to be "attracted" to lacunae inside the cloud as well as to cells actively absorbing nutrient molecules. The net over-all effect, however, would be to generally decrease the nutrient delivery to the phytoplankton cells within the microcloud, in direct competition with the nutrient enhancement described in the preceeding section. The net result of these two opposing effects is an important issue that is beyond the scope of this paper.

5.3 Future directions.

Thus we have established the plausibility of the existence of a microcloud structure mediating the transformation of exuded DOC into secondary production. Perhaps more importantly, we have shown how this transformation can be modulated by physical forcing associated with the turbulent kinetic energy dissipation rate. This is of course remarkable because it links very large scale processes such as the wind field directly with the smallest scale processes that relate to diffusion and turbulent flow.

Future research would include the development of laboratory and field experiments to test the theory. Additional theoretical developments would include understanding how the geometry of clouds is affected by the dynamics of the flow field and the properties of diffusion.

5.4 Acknowledgements.

6.0 REFERENCES

Baines, S.B. and M.L. Pace (1991) The Production of Dissolved Organic Matter by Phytoplankton and its Importance to Bacteria: Patterns across Marine and Freshwater Systems. *Limnology and Oceanography,* **36**(6), 1078–1090.

Batchelor, G.K. (1959) Small-Scale Variation of Convected Quantities like Temperature in Turbulent Fluid. Part 1. General discussion and the case of small conductivity. *Journal of Fluid Mechanics,* **5**, 113–133.

Bell, W. and R. Mitchell (1972) Chemotactic and Growth Responses of Marine Bacteria to Algal Extracellular Products. *The Biological Bulletin,* **143**(2), 265–277.

Bowen, J.D., K.D. Stolzenbach and S.W. Chisholm (1993) Simulating bacterial clustering around phytoplankton cells in a turbulent ocean. *Linmology and Oceanography,* **38**(1), 36–51.

Chisholm, S.W. (1992) Phytoplankton Size. in *Primary Productivity and Biogeochemical Cycles in the Sea.* P.G. Falkowski and A.D. Woodhead eds., *Plenum Press,* New York, 213–237.

Cressie, N.A.C. (1993) Statistics for Spatial Data. *J. Wiley,* New York, 900 p.

Denman, K.L. and A.E. Gargett (1995) Biological–Physical Interactions in the Upper Ocean: The Role of Vertical and Small Scale Transport Processes. *Annu. Rev. Fluid Mech.,* **27**, 225–255.

Fenchel, T. (1988) Marine Plankton Food-Chains. *Annual Review of Ecology and Systematics,* **19**, 19–38.

Hulburt, E.M. (1970) Competition for Nutrients by Marine Phytoplankton in Oceanic, Coastal and Estuarine Regions. *Ecology,* **51**(3), 475–484.

Kahru, M., E. Kaasik and A. Leeben (1991) Annual Cycle of Partical Size Fractions and Phytoplankton Biomass in the Northern Baltic Proper. *Marine Ecology Series,* **69**, 117–124.

Lazier, J.R.N. and K.H. Mann (1989) Turbulence and the Diffusive Layers Around Small Organisms. *Deep Sea Research,* **36**(11), 1721–1733.

Mitchell, J.G., A. Okubo and J.A. Fuhrman (1985) Microzones Surrounding Phytoplankton Form the Basis for a Stratified Marine Microbial Ecosystem. *Nature,* **316**(6023), 58–59.

Munk, W.H. and G.A. Riley (1952) Absorption of Nutrients by Aquatic Plants. *Journal of Marine Research,* **11**, 215–240.

Pasciak, W.J. and J. Gavis (1974) Transport Limitation of Nutrient Uptake in Phytoplankton. *Limnology and Oceanography,* **19**(6), 881–888.

Richardson, L.L. and K.D. Stolzenbach (1995) Phytoplankton cell size and the development of microenvironments. *FEMS Microbiology Ecology,* **16**, 185–192.

Rothschild, B.J. (1992) Application of Stochastic Geometry to Problems in Plankton Ecology. *Philosophical Transactions of the Royal Society of London Series B-Biological Sciences,* **336**(1277), 225–237.

Rothschild, B.J. and T.R. Osborn (1988) Small-Scale Turbulence and Plankton Contact Rates. *Journal of Plankton Research,* **10**(3), 465–474.

Stoyan, D., W.S. Kendall and J. Mecke (1987) Stochastic Geometry and its Applications. *J. Wiley*, New York, 345 p.

Sundby, S. and P. Fossum (1990) Feeding Conditions of Arcto-Norwegian Cod Larvae Compared with the Rothschild-Osborn Theory on Small-Scale Turbulence and Plankton Contact Rates. *Journal of Plankton Research,* **12**(6), 1153–1162.

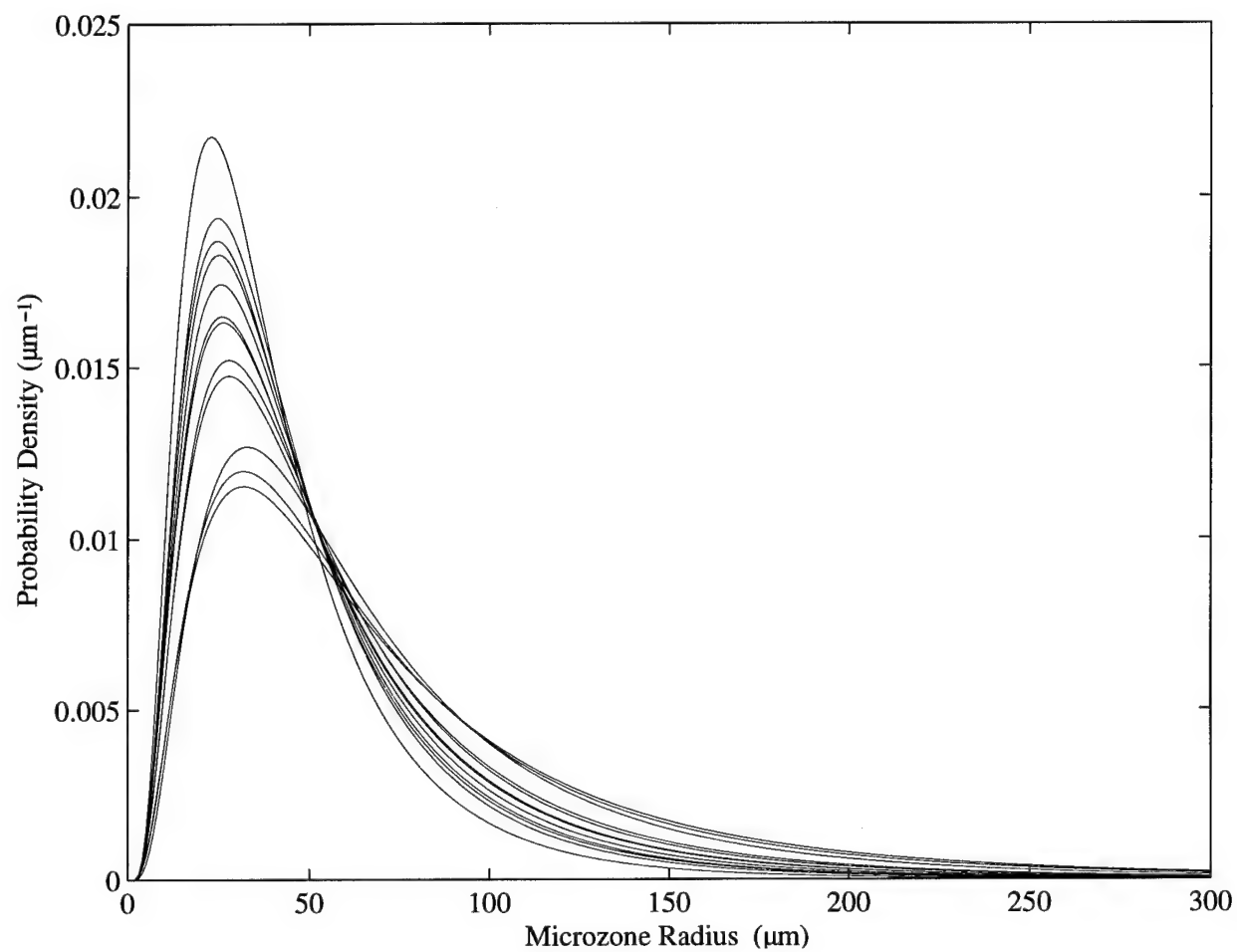Tennekes, H. and J.L. Lumley (1972) A First Course in Turbulence. *MIT Press*, Cambridge, 300 p.

Figure 1 Probability density curves. The data of Kahru *et al.* (1991) fit to the log-normal distribution. Each curve refers to a 10 day period in the data.
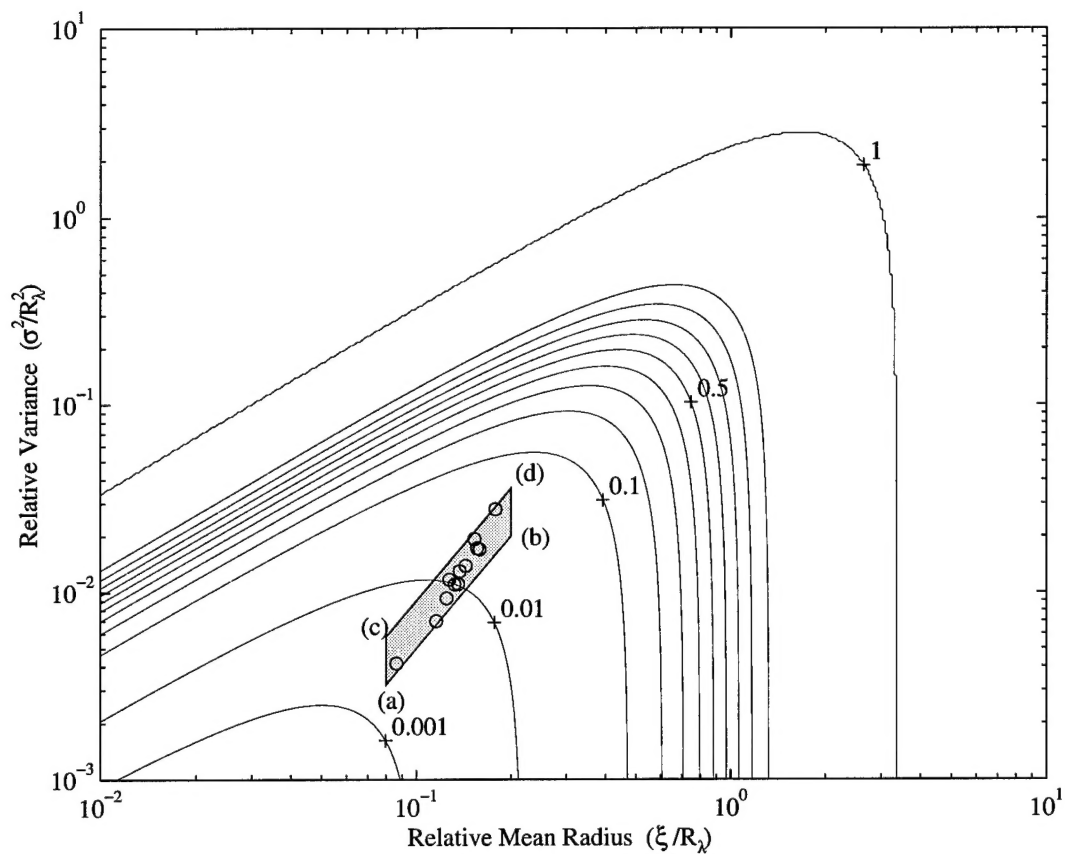
Figure 2 Volume fraction contours. The volume fraction occupied by the ensemble microzone. The circles indicate the position in parameter space for the Kahru *et al.* (1991) data. The shaded region is the "reference" area suggested by the Kahru *et al.* data.
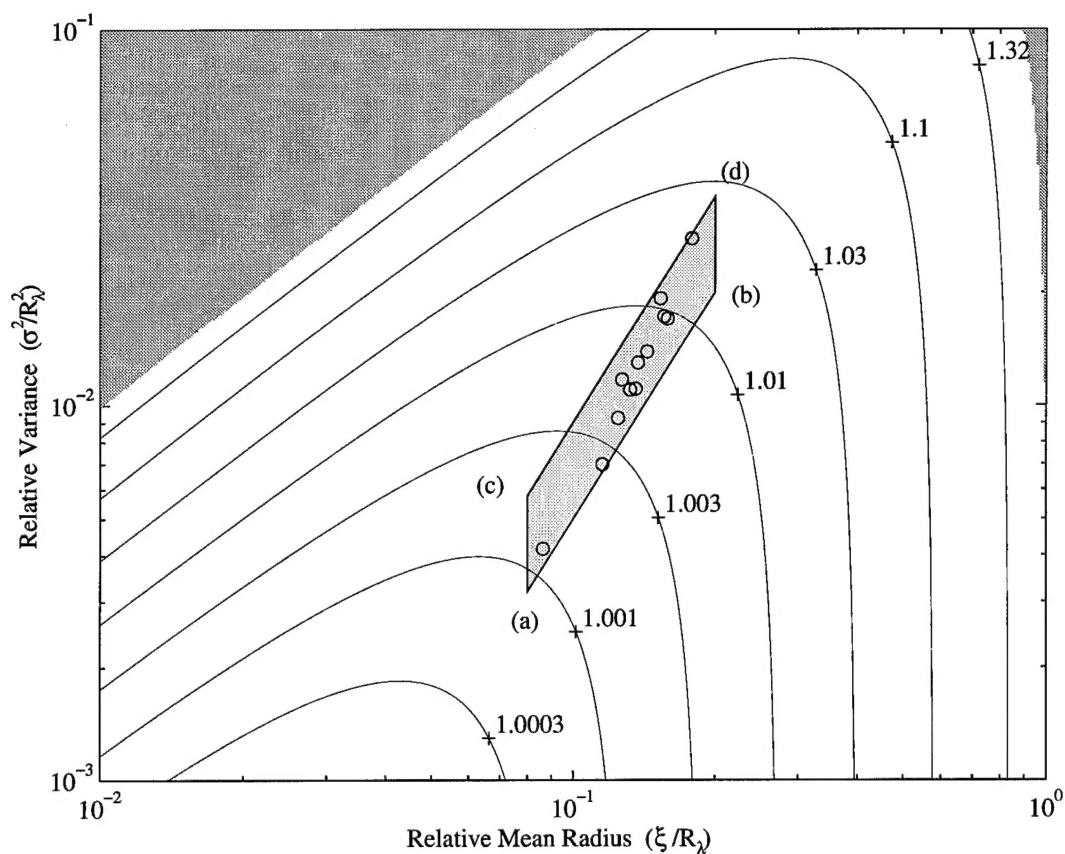
Figure 3 Concentration factor contours. An upper bound for the concentration effect due to the overlapping of the microzones. The circles indicate the position in parameter space for the Kahru *et al.* (1991) data. The light gray shaded region is the "reference" area suggested by the Kahru *et al.* data. The dark gray shaded regions in the upper corners are parameter regimes in which the microzones must overlap.
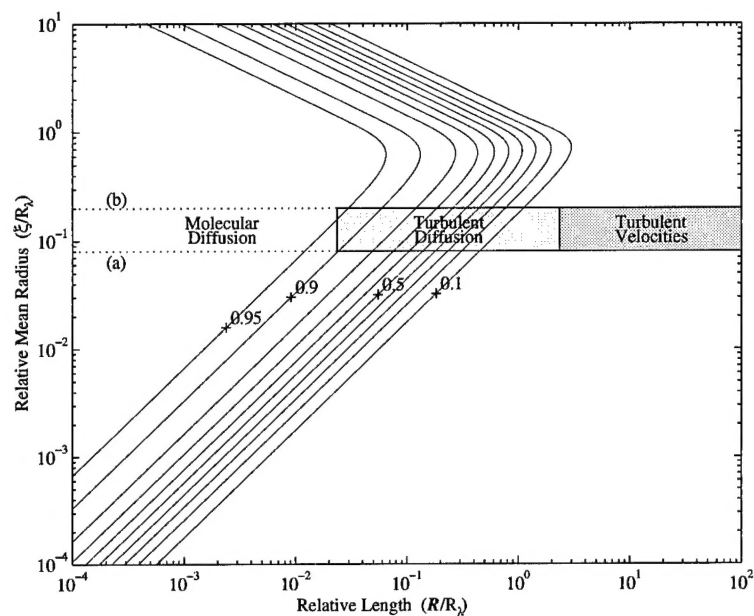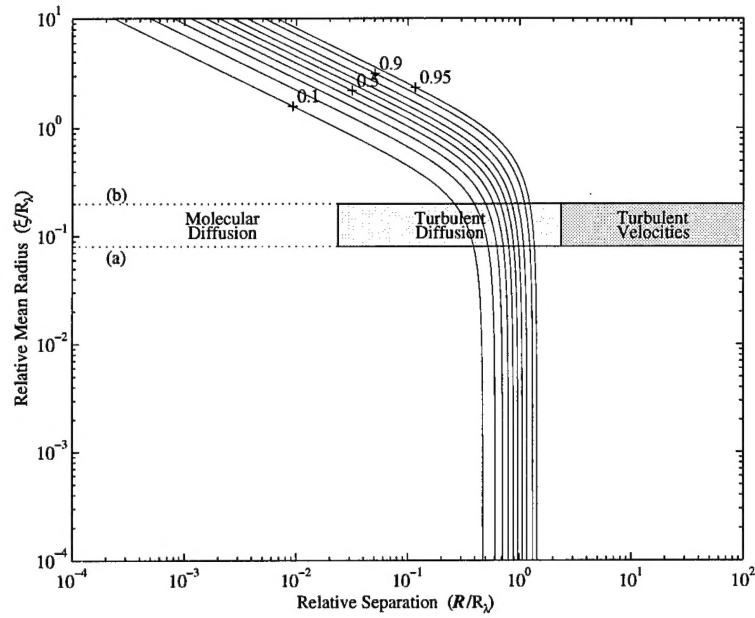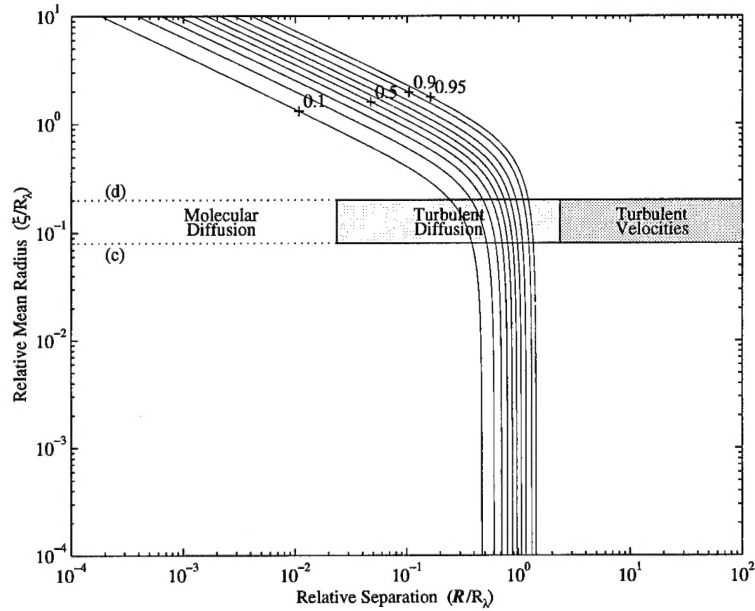
(a)
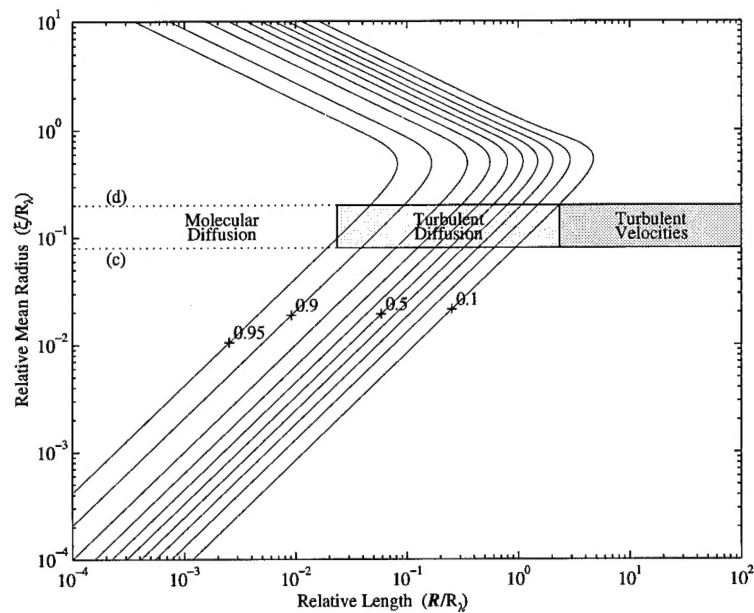
(b)

Figure 4 Correlation contours for (a) $\sigma^2 = 0.5\xi^2$ and (b) $\sigma^2 = 0.9\xi^2$. Dotted lines delimit ranges for phytoplankton microzone mean radii of the Kahru *et al.* (1991) data, corresponding to points (a)–(d) in figure 2.

(a)

(b)

Figure 5 Spherical contact distribution contours for (a) $\sigma^2 = 0.5\xi^2$ and (b) $\sigma^2 = 0.9\xi^2$. Dotted lines delimit ranges for phytoplankton microzone mean radii of the Kahru *et al.* (1991) data, corresponding to points (a)–(d) in figure 2.